NUKLEONIKA 2008;53(1):3–6

ORIGINAL PAPER

Assessment of a new scintillation crystal ($LaBr_3$) in PET scanners using Monte Carlo method

Ali R. Karimian,
Christopher J. Thompson

Abstract. The main aim of this work is to investigate the use of new lanthanum bromide ($LaBr_3$) in whole body PET (WB-PET) scanners and to compare the obtained results with those for BGO and LSO crystals which are currently used in conventional and dedicated PET systems. Our results show that there is a gain in noise effective count rate (NECR) arising from the reduced scatter and random fractions in a $LaBr_3$ scanner. The spatial resolution of the WB-PET with $LaBr_3$ is slightly worse than the LSO and BGO crystals because of its low density and effective atomic number. But our study showed the increased NECR, excellent energy resolution and low decay time of $LaBr_3$ which promise a significant improvement in WB-PET performances especially for narrow coincidence windows.

Key words: PET • scintillation crystals • Monte-Carlo • lanthanum bromide

A. R. Karimian✉
Biomedical Engineering Group,
Engineering Faculty,
University of Isfahan,
Isfahan, Postal code: 81744, Iran,
Tel.: +98 311 793 2773, Fax: +98 311 793 2771,
E-mail: karimian@eng.ui.ac.ir

C. J. Thompson
Montreal Neurological Institute – McGill University,
3801 University Str. #798,
Montreal QC H3A-2B4, Canada

Received: 27 July 2007
Accepted: 1 October 2007

Introduction

PET (positron emission tomography) is a powerful and sensitive technique for functional imaging in the field of nuclear medicine. Inorganic scintillator crystals are the most commonly used detectors for PET systems. The choice of the scintillator is a fundamental element of a PET design [3]. The current generation of conventional whole body PET and also dedicated PET scanners are using mostly BGO (bismuth germinate), LSO (lutetium oxyorthosilicate) and GSO (gadolinium oxyorthosilicate) detectors. Recently cerium doped lanthanum bromide ($LaBr_3$:Ce), developed by Saint Gobain (France), has been suggested for use in PET systems [8, 9]. Table 1 summarizes the important properties for selected scintillators which are currently in use or under development for PET applications [1, 3, 4, 8, 9]. The advantages of $LaBr_3$, in comparison to BGO, LSO and GSO as shown in Table 1, are: high light yield (more than 2.1 times over LSO and about 7 times over BGO and GSO), its excellent energy resolution (2.9%) which is about 35% for the other scintillation crystals.

Also the low melting point of the $LaBr_3$ scintillator (783°C) suggests that in the long run this scintillator can be cost-effective [1, 4, 8–10]. The shortcomings of $LaBr_3$, in comparison to BGO, LSO and GSO, are: its photofraction is about 46% of the LSO, 60% of GSO and 36% of BGO; its density and effective atomic number are about 70% and 60% of the other crystals, respectively, and furthermore $LaBr_3$ is hygroscopic.

Table 1. Characteristics of scintillator crystals under development and currently used in commercial and prototype PET tomographs design [1, 3, 4, 8, 9]

Scintillator	BGO	LSO	GSO	$LaBr_3$
Density (g/cc)	7.13	7.4	6.71	5.29
Light yield (photons/keV)	9	30	8	63
Effective *Z*	75	66	60	46.9
Principal decay time (ns)	300	42	30–60	16
Peak wavelength (nm)	480	420	440	358
Index of refraction	2.15	1.82	1.95	1.88
Photo fraction (%)[a]	41.5	32.5	25	15
Attenuation length (cm)[a]	1.04	1.15	1.42	2.13
Energy resolution (%)[a]	7.9	8	6.9	2.9
Hygroscopic	no	no	no	yes

[a] at 511 KeV

In this investigation, because of the above mentioned advantages and shortcomings of $LaBr_3$, we were trying to predict by the Monte Carlo method some important parameters of WB-PET systems such as: NECR max (noise equivalent count rate), scatter fraction, tangential and radial spatial resolution of the WB-PET system when its crystals are one of the BGO, LSO or $LaBr_3$ in each study.

Materials and methods

To assess the important parameters such as: NECR max scatter fraction, tangential and radial spatial resolution of the WB-PET system a currently available conventional WB-PET system (GE Advance, GEMS, Milwaukee WI), whose performance characteristics were available to us, was used. The GE Advance WB-PET consists of 12,096 bismuth germinate (BGO) crystals (30 mm (radial) × 8.1 mm (axial) × 4 mm (transaxial)) which are grouped in detector blocks of 6 × 6 crystals each, with 18 rings and a transaxial FOV (field of view) of 55 cm, an axial FOV of 15.2 cm with a ring diameter of 92.7 cm and a patient port of 59 cm [2]. This study was done when the crystals of GE Advance WB-PET system are one of the BGO, LSO or $LaBr_3$ in each study.

When the performance of PET scanners is reported, it is often done by the reference to a standard phantom proposed by the National Electrical Manufacturers Association of the USA (NEMA). Therefore, in this research we used a NEMA standard Lucite cylindrical phantom and the Monte Carlo simulation programming package: PETSIM [2, 5–7, 11, 12].

These programs simulate the source fluence, then the events which pass through the collimator, and finally those rays which are detected in separate files. Each γ-ray requires 20 bytes of storage. The simulation data files consist of blocks containing 256 γ-rays. Generally, in simulation programs, higher numbers of simulated counts give better precision and signal to noise ratio and image quality because of lower statistical noise. Therefore, to reduce the effects of statistical noise on the output results of simulations in this research, a maximum number of output blocks which could be saved (i.e. 100,000 blocks) was used for gamma-ray history file (GRH) of "phantom" program and for other programs in PETSIM, namely "collimator" and "detector". The GRH files were selected proportionally to this maximum number of blocks.

To compare the performance of each study with one of the BGO, LSO or $LaBr_3$ scintillation crystals, the NEMA standard phantom was used. The NECR of the WB-PET system were estimated over the range of activity concentrations and was calculated from the following formula:

$$\text{NECR} = T^2/(T + S + 2R) \quad (1)$$

where: *T* is the true coincidence rate; *R* is the random coincidence rate; *S* is the scatter coincidence rate [3].

The top view of WB-PET with the NEMA phantom inside, its patient port and the used scintillation crystal material $LaBr_3$ (as an example in our study) is shown in Fig. 1.

The considered standard settings for WB-PET (GE Advance) with the BGO, LSO and $LaBr_3$ scintillation crystals were listed in Table 2.

The listed settings inside Table 2 were selected from the performance characteristics of the current PET scanners and experimental data [1, 5, 6, 10]. Although very narrow coincidence windows, i.e. 1 and 2 ns, are not used now in practice because of the limitations in the electronic and detection systems, but to complete

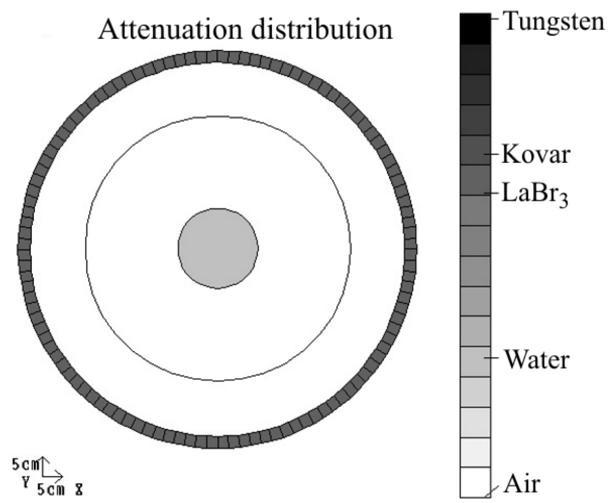

Fig. 1. Top view of simulated WB-PET with $LaBr_3$ scintillation crystals and standard NEMA phantom located in its center. The blackening is proportional to the linear attenuation coefficient of materials.

Table 2. The standard settings which were considered for WB-PET (GE Advance) with different kinds of scintillation materials

Scintillation material	Coincidence window (ns)	Dead time (μs)	Energy resolution (%)	Energy discriminator (keV)	
				Lower level	Upper level
BGO	12.5	3.6	20	300	650
LSO	1,2,4,6	0.5	20	300	650
$LaBr_3$	1,2,4,6	0.3	11	300/400	650

our simulation and to see the effect of very narrow coincidence window on performance characteristics of WB-PET systems also this simulations have been done.

The scatter fraction (SF) is a principal factor affecting the image contrast and image quantitation. It was calculated for all the three scintillation materials in this research by using the output data of Monte Carlo simulation and using the following formula:

(2) Scatter fraction (SF) $= S/(S + T)$

In this formula S represents the scattered counts and T the true counts [3, 12].

In order to estimate the spatial resolution of the WB-PET system in the 3D mode with BGO, LSO and $LaBr_3$ scintillation materials we again used PETSIM. The resolution module in PETSIM works best when a uniform source is used, as opposed to several very small sources which would be most accurate in a real experiment [5, 6, 11, 12]. The resolution experiments were done with an air-filled cylinder to minimize scattering of gamma rays, thus improving the storage and time efficiency of the program. The positron range can be set to that of F-18 in water, so that the effects of positron range can be included in the simulation.

The file contains exact location of each positron emitting nucleus, thus the programs can estimate a normal distance between the lines of response corresponding to that joining the centers of the two crystals in which the annihilation photons interact the location of the nucleus. In this case we assumed ^{18}F positrons, non-co linearity of 0.51 degrees [3, 12], and divided the field into five radial bins. For this purpose, an air cylinder with a diameter of 50 cm was simulated inside the WB-PET to cover the entire imaging FOV of the system. The mean radii of the bins (the position of point sources) were: 2.5, 7.5, 12.5, 17.5, 22.5 cm for WB-PET. The resolution measurements were done for BGO, LSO and $LaBr_3$ scintillation materials by including the effects of both positron ranges and annihilation photon non-co linearity for all the simulations.

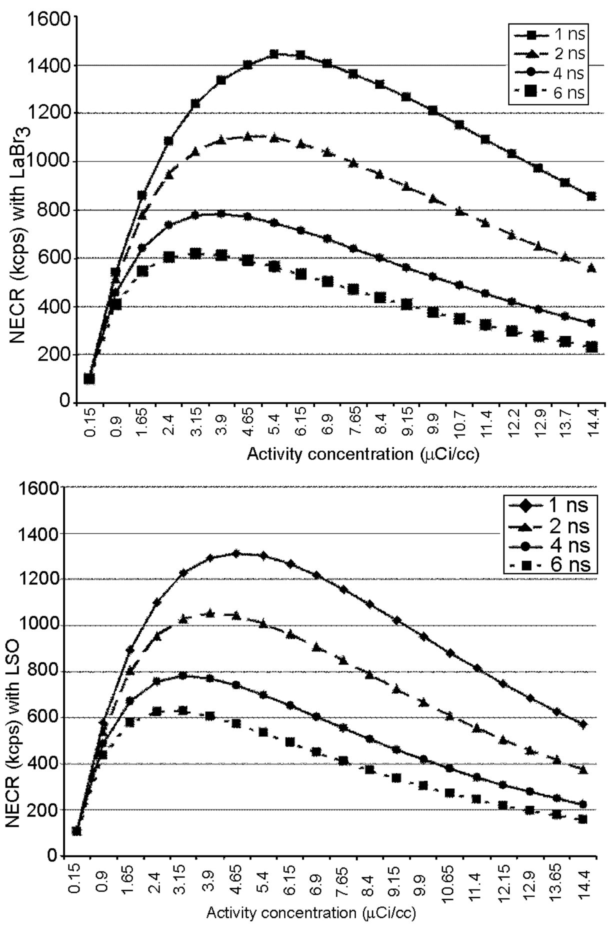

Fig. 2. NECR curves for WB-PET (GE Advance) by using a standard Lucite cylindrical phantom (20 cm ID, 18.5 cm length), simulation results by PETSIM for $LaBr_3$ (top) and LSO (bottom) scintillation crystals.

Results

In our pervious work we demonstrated that PETSIM has a very good ability for studying the NECR of PET systems in 2D and 3D modes [5, 6, 11]. The simulation results of the conventional WB-PET system (GE Advance) in 3D mode for $LaBr_3$ and LSO scintillation crystals by using a standard Lucite cylindrical phantom (20 cm ID, 18.5 cm length) are shown in Fig. 2.

The NECR max of WB-PET with BGO crystal and 12.5 ns coincidence window was 250 Kcps.

The scatter fraction (SF) of the WB-PET system with different types of scintillation crystals and different lower/upper level (LLD/ULD) discriminator of energy are shown in Table 3. Also one set of the curves whose data were used to calculate the scatter fraction and to show the true and scatter coincidences is shown in Fig. 3.

Table 3. Scatter fraction of the WB-PET system by using the standard NEMA phantom and a different setting for lower/upper level energy of a discriminator

Scintillation material	LLD	ULD	SF
BGO	300	650	0.259
LSO	300	650	0.265
$LaBr_3$	300	650	0.268
$LaBr_3$	400	650	0.230

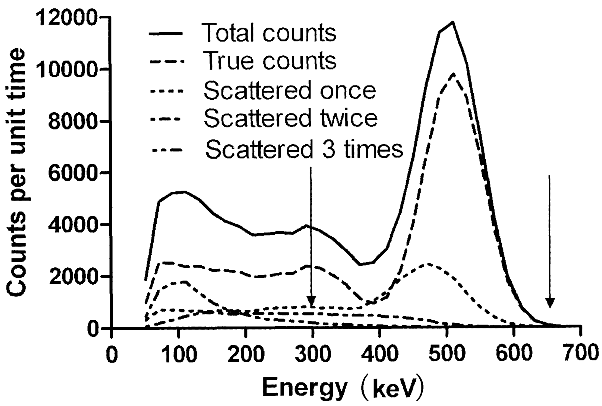

Fig. 3. True and scatter coincidence events curves in the WB-PET system with $LaBr_3$ and using the NEMA standard phantom. The arrows show setting for lower and upper level energy of a discriminator.

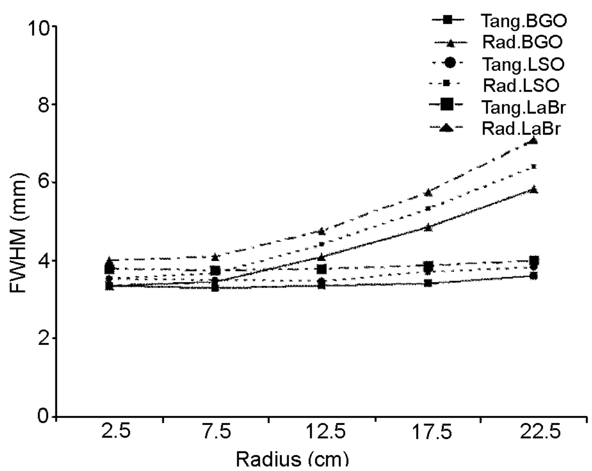

Fig. 4. Radial and tangential components of spatial resolution for WB-PET with different kinds of scintillation crystals by simulation.

Assessment of resolution for WB-PET with different scintillation materials is presented in Fig. 4. The results show that the tangential and radial resolutions of WB-PET system with $LaBr_3$ crystals are slightly worse than those for LSO crystals, i.e. about 4% for tangential and 10% for radial resolution, inside a wide 45 cm field of view (FOV).

Conclusion

The results show that the NECR max (noise equivalent count rate) of the WB-PET system with the $LaBr_3$ crystal were about 1449, 1115, 792, 623 Kcps in comparison with LSO whose NECR max were 1312, 1054, 781, 628 Kcps for the coincidence window of 1, 2, 4, 6 ns, respectively. The NECR max of WB-PET with the BGO crystal and 12.5 ns coincidence window was 250 Kcps.

Also, because of the possibility to use a narrow coincidence window for $LaBr_3$, in comparison to LSO and BGO, due to its small decay time (16 ns for $LaBr_3$, for LSO and BGO are 42 and 300 ns, respectively) the random rates of $LaBr_3$ is smaller than the other scintillation crystals which cause the improved NECR. Furthermore, a shorter decay time of $LaBr_3$, in comparison to LSO and BGO, is leading to a reduced pulse pile-up in the scanner.

Meanwhile, because of the excellent energy resolution of $LaBr_3$ it would be possible to use a higher LLD which improves its scatter fraction.

Our study shows the spatial resolution of WB-PET system with the $LaBr_3$ crystal is slightly worse than that of LSO and BGO crystals. But the advantages of $LaBr_3$ which are: high light yield (more than 2.1 times over LSO and about 7 times over BGO), excellent energy resolution (2.9%) which is about 30–40% of the other mentioned scintillation crystals and decay time which is about 5% and 38% of BGO and LSO, respectively and the outcomes from this study promise that $LaBr_3$ can potentionally introduce a significant improvement into WB-PET performances, especially for narrow coincidence windows.

Acknowledgment. The authors wish to thank the University of Isfahan for supporting this research by the IU grant.

References

1. Braem A, Chamizo Llatas M, Chesi E *et al.* (2004) Feasibility of a novel design of high resolution parallax-free Compton enhanced PET scanner dedicated to brain research. Phys Med Biol 49:1–16
2. DeGrado TR, Turkington TG, Williams JJ, Stearns CW, Hoffman JM, Coleman RE (1994) Performance characteristics of a whole-body PET scanner. J Nucl Med 35:1398–1405
3. Humm JL, Rosenfeld A, Del Guerra A (2003) From PET detectors to PET scanners. Eur J Nucl Med 30:1574–1597
4. Karimian A, Thompson CJ (2006) Assessment of using new scintillation crystal ($LaBr_3$) in PET system by Monte Carlo method. In: World Congress on Medical Physics and Biomedical Engineering, August 27 – September 1, 2006, Seoul, Korea, pp 1584–1586
5. Karimian A, Thompson CJ, Sarkar S *et al.* (2004) A dedicated PET system for breast imaging (CYBPET), M2-1. IEEE NSS MIC, Rome, Italy (CD edition)
6. Karimian A, Thompson CJ, Sarkar S *et al.* (2005) CYBPET: A cylindrical PET system for breast imaging. Nucl Instrum Methods Phys Res A 545:427–435
7. NEMA (2001) Performance measurements of positron emission tomographs. NEMA Standards Publication NU 2 – 1994 & 2000. National Electrical Manufacturers Association, Rosslyn
8. Rozsa CM, Mayhugh MR, Menge PR, Rothan D, Dathg C (2006) Brilliance scintillators $LaCl_3$(Ce) and $LaBr_3$(Ce): recent advances and results, Saint-Gobain Crystals. IEEE MIC, San Diego, CA, USA
9. Saint-Gobain Crystals, Saint-Gobain Ceramics & Plastics, Inc. (2004) BrilLanCe™380 [$LaBr_3$(Ce)] data sheet, http://www.detectors.saint-gobain.com/
10. Surti S, Karp JS, Muehllehner G, Raby PS (2003) Investigation of lanthanum scintillator for 3-D PET. IEEE Trans Nucl Sci 50:348–354
11. Thompson CJ, Moreno-Cantu J, Picard Y (1992) PETSIM: Monte Carlo simulation of all sensitivity and resolution parameters of cylindrical positron imaging systems. Phys Med Biol 37:731–749
12. Thompson CJ, Picard Y (2003) PETSIM Monte Carlo simulation programs guide to writing batch processing command files. Revision 2003